Identification of Essential Residues of Human α-L-Fucosidase and Tests of Its Mechanism†

Sheng-Wen Liu,‡,§ Chao-Sheng Chen,‡,§ Shih-Shen Chang,§ Kwok-Kong Tony Mong,§ Chun-Hung Lin,|| Cheng-Wen Chang,⊥ Chuan Yi Tang,⊥ and Yaw-Kuen Li*,§

Department of Applied Chemistry, National Chiao Tung University, Institute of Biological Chemistry, Academia Sinica, and Department of Computer Science, National Tsing Hua University, Hsinchu, Taiwan

Received August 13, 2008; Revised Manuscript Received November 4, 2008

ABSTRACT: Fucosylated glycoconjugates have critical roles in biological processes, but a limited availability of α-L-fucosidase has hampered research on this human enzyme (h-Fuc) at a molecular level. After overexpressing h-Fuc in *Escherichia coli* as an active form, we investigated the catalytic function of this recombinant enzyme. Based on sequence alignment and structural analysis of close homologues of h-Fuc, nine residues of glutamate and aspartate in h-Fuc were selected for mutagenic tests to determine the essential residues. Among the mutants, D225N, E289Q, and E289G lost catalytic activity significantly; their k_{cat} values are 1/5700, 1/430, and 1/340, respectively, of that of the wild-type enzyme. The Brønsted plot for k_{cat}/K_m for the E289G mutant is linear with $\beta_{lg} = -0.93$, but that for k_{cat} is biphasic, with β_{lg} for poor substrates being −0.88 and for activated substrates being −0.11. The small magnitude of β_{lg} for the activated substrates may indicate that the rate-limiting step of the reaction is defucosylation, whereas the large magnitude of the latter β_{lg} value for the poor substrates indicates that the rate-limiting step of the reaction becomes fucosylation. The kinetic outcomes support an argument that Asp^{225} functions as a nucleophile and Glu^{289} as a general acid/base catalyst. As further evidence, azide significantly reactivated D225G and E289G, and ^{1}H NMR spectral analysis confirmed the formation of β-fucosyl azide and α-fucosyl azide in the azide rescues of D225G and E289G catalyses, respectively. As direct evidence to prove the function of Glu^{289}, an accumulation of fucosyl-enzyme intermediate was detected directly through ESI/MS analysis.

Fucose-containing carbohydrates are involved in such critical physiological activities as oncogenesis (*1, 2*), blood coagulation cascade and clot dissolution (*3*−*5*), and host-microbial interactions (*6, 7*). α-L-Fucosidases (EC 3.2.1.51) are responsible for the removal of L-fucosyl residues from the nonreducing end of glycoconjugates. A severe deficiency of α-L-fucosidase causes fucosidosis that can produce mental and motor retardation (*8*). Several pathological conditions including inflammation (*4, 9*), cancer (*10*−*12*) and cystic fibrosis (*13, 14*) are also related to an atypical activity of α-L-fucosidase. Human α-L-fucosidases (h-Fuc)[1] are thus of substantial interest because abnormal fucosidase activity in serum was shown to serve as a diagnostic marker of early colorectal (*2, 12*) and hepatocellular cancers (*10, 15*). A treatment of α-L-fucosidase to breast cancer cells also showed impairment of the interaction between these tumor cells and their microenvironment, which might consequently modulate metastasis (*16*).

α-L-Fucosidases occur commonly in nature with varied substrate specificities. Those from mammalian tissues and marine gastropods have broad substrate specificity: they cleave α1−2 linkages to galactose and α1−3, α1−4, and α1−6 linkages to *N*-acetylglucosamine (*17*−*19*), whereas the enzymes from microorganisms and almond emulsion remove only the α1−2 linkage to a galactose (*20, 21*). All known retaining α-L-fucosidases are classified into the glycoside hydrolase family 29 (GH-29), whereas the inverting α-L-fucosidases are grouped in GH-95 (http://www.cazy.org/fam/ acc_GH.html) (*22*).

Human α-L-fucosidases have been purified from various cells, fluids, and tissues; their kinetic, electrophoretic, and immunological properties were reported (*23*). In general, h-Fuc is a multimeric protein derived from two closely related polypeptide subunits of mass ∼50−60 kDa and has variable carbohydrate composition and possibly other post-translational modifications (*24*−*26*). α-L-Fucosidase from blood plasma is a sialoglycoprotein that contains ∼7−8% carbohydrate by mass. Although the exact functions of the carbohydrate component are ambiguous, not only the stability and kinetic properties of the enzyme but also the protein

† The MOE-AU program of Taiwan and the National Science Council of Taiwan (Contract NSC95-2113-M-009-004) provided financial support.

* Address correspondence to this author. Tel: 886-3-5731985. Fax: 886-3-5723764. E-mail: ykl@faculty.nctu.edu.tw.

‡ These authors contributed equally to this work.

§ National Chiao Tung University.

|| Academia Sinica.

⊥ National Tsing Hua University.

[1] Abbreviations: CNPF, 2-chloro-4-nitrophenyl α-L-fucopyranoside; PF, phenyl α-L-fucopyranoside; pCPF, *p*-cyanophenyl α-L-fucopyranoside; mNPF, *m*-nitrophenyl α-L-fucopyranoside; pNPF, *p*-nitrophenyl α-L-fucopyranoside; MeNPF, 2-methyl-4-nitrophenyl α-L-fucopyranoside; FNPF, 2-fluoro-4-nitrophenyl α-L- fucopyranoside; TAF, 2,3,4-tri-*O*-acetyl-L-fucopyranosyl 2,2,2-trichloroacetimidate; h-Fuc, human α-L-fucosidase; Tm-Fuc, *Thermotoga maritima* α-L-fucosidase.

10.1021/bi801529t CCC: $40.75
Published on Web 12/12/2008

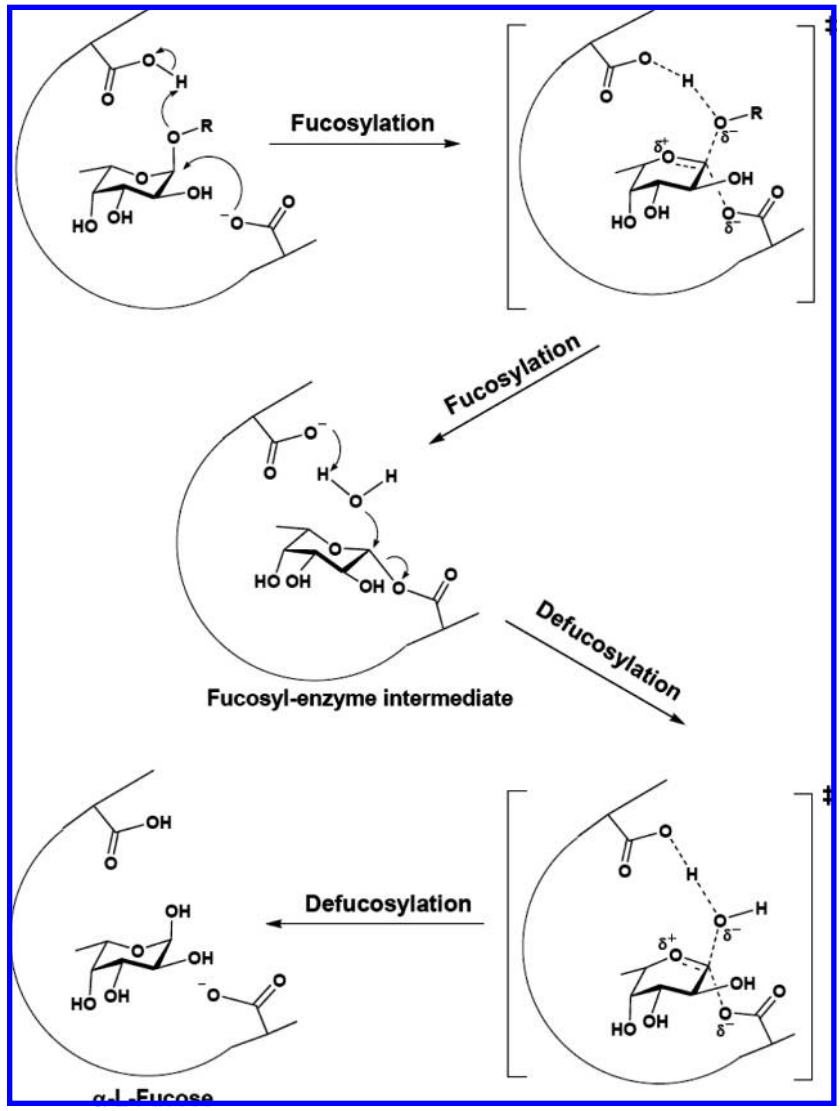

FIGURE 1: Proposed mechanism of α-L-fucosidase. A two-step, double-displacement mechanism is proposed involving two essential amino acid residues, one functioning as a nucleophile and another as a general acid/base.

folding, intracellular transport, secretion, and generation of multiple molecular forms are suggested to be influenced by the level of glycosylation (*27*−*29*).

cDNA clones containing the coding sequence of *h-fuc* were isolated and identified (*30*−*32*). The open reading frame encodes human liver tissue α-L-fucosidase having 461 amino acids and containing a signal peptide with 22 amino acids (*30*). The expression of the recombinant enzyme was reported only as a fusion protein forming an inclusion body (*33*). Because of a lack of this enzyme and of the complicated substrate synthesis, a detailed catalytic mechanism and the essential residues of h-Fuc involved in the catalysis have been little investigated (*34*). h-Fuc from liver is a retaining enzyme (*35*). Moreover, α-L-fucosidase from *Thermus* sp. Y5 (*36*), *Pecten maximus* (*37*), *Sulfolobus solfataricus* (Ss-Fuc) (*38*), and *Thermotoga maritima* (Tm-Fuc) (*39*) were proved to possess the same catalytic preference. Two key active site carboxylic acid residues are involved in the catalytic reaction and utilize a double displacement mechanism in which an α-L-fucosyl intermediate is formed and hydrolyzed. Both steps proceed via transition structures with substantial oxocarbonium ion character (*40*); a proposed mechanism appears in Figure 1. In the first step (fucosylation), one carboxylic acid residue serving as a nucleophile attacks the anomeric carbon of the fucoside, while another acting as an acidic catalyst protonates the fucosidic oxygen, thereby promoting the leaving of the aglycon moiety; thus is formed a covalent fucosyl-enzyme intermediate. In the second step (defucosylation), the general acid becomes a general base that assists the decomposition of the fucosyl-enzyme intermediate, proceeding through a general base-catalyzed attack of water at the anomeric center to release the fucose. The identification of these catalytic essential residues is of primary importance for an understanding of the detailed mechanism at a molecular level on which these enzymes function. Kinetic analysis of artificial substrates, each with a glycose moiety attached to a leaving phenol, is generally employed to investigate the enzymatic catalysis in detail. An extended Brønsted relationship is typically measured. As enzymes in the same family possess a presumably similar catalytic mechanism (*41*), solving the mechanistic action of a particular enzyme might help in understanding the reaction pattern of the family.

In this work, we overexpressed human α-L-fucosidase in *Escherichia coli* as an active form and developed an effective method to synthesize artificial substrates. Tm-Fuc is the

closest bacterial relative of mammalian α-L-fucosidase of which the crystal structure has been determined (*42*). Although Tm-Fuc shares 38% sequence identity with its human counterpart, we found the residues responsible for the catalytic acid/base not to be conserved for these two enzymes. Equipped with structural information of Tm-Fuc, we used a sequence alignment of close homologues of h-Fuc to select rationally the candidates for mutagenesis. Combined with site-directed mutagenesis and kinetic experiments, the catalytic function and the essential residues of h-Fuc were examined and identified.

EXPERIMENTAL PROCEDURES

Search for Candidates of Catalytic Essential Residues. In addition to human and *T. maritima*, in total six UniProt (*43*) annotated animal fucosidases from CAZy GH-29 with sequence identity less than 70% were selected for sequence analysis. The UniProt accession numbers of the studied fucosidases are *T. maritima* Q9WYE2 (Tm-Fuc), *Halocynthia roretzi* Q8TA71 (Hr-Fuc), *Schistosoma japonicum* Q86FH9 (Sj-Fuc), *Pongo abelii* Q5RFI5 (Pa-Fuc), *Drosophila melanogaster* Q9VTJ4 (Dm-Fuc), *Caenorhabditis elegans* P49713 (Ce-Fuc), and *Dictyostelium discoideum* P10901 (Dd-Fuc). As the tested h-Fuc differs slightly from the corresponding UniProt P04066, the position of a residue is specified according to NCBI M29877. The boundaries of the TIM barrel domain (IPR017853) of each protein were set based on the InterPro database (http://www.ebi.ac.uk/interpro/). The multiple sequence alignment of fucosidases was performed with a Praline server and options of a standard progressive strategy and a PSIPRED-based secondary structure prediction (http://zeus.cs.vu.nl/programs/pralinewww/). The propensity of the PSIPRED β-strand (or α-helix) was defined as the ratio of the number of predicted E (or H) to the number of h-Fuc close homologues ($n = 7$) within an aligned column. The 3D structure of h-Fuc was predicted using the Swiss-model server (http://swissmodel.expasy.org/) with default settings. A comparison of the predicted h-Fuc structure and Tm-Fuc was performed with the combinatorial extension (CE) method (http://cl.sdsc.edu/). The Cα−Cα distance between Tm-Fuc D224 and selected Glu/Asp was obtained on averaging the distances calculated from PDB 1odu, 1hl8, and 1hl9. A residue near the end of the β-strand of the TIM barrel with its equivalent Tm-Fuc Cα−Cα distance less than 20 Å was identified as a candidate for catalytic essential residues.

Materials. Vector pCMV.SPORT6 containing a human tissue α-L-fucosidase gene (*h-fuc*) (NCBI accession number M29877) (Stragene, La Jolla, CA), pET vector system (Invitrogen, Carlsbad, CA), *Vent* DNA polymerase (New England Biolabs, Ipswich, MA) for PCR reactions, restriction endonucleases and T4 DNA ligase (Roche Applied Science, Basel, Switzerland), protein marker standards of small molecular mass for electrophoresis (GE Healthcare, Piscataway, NJ), buffers and chemicals for synthesis (Sigma-Aldrich, St. Louis, MO, or E. Merck, Gibbstown, NJ), and columns and gels for protein purification (GE Healthcare) were obtained from the indicated sources. Synthetic substrates were characterized with ^{1}H NMR (300 MHz, Bruker Avance) and mass (positive ESI mode, QTOF; Micromass, Manchester, U.K.) spectra.

Reconstruction of Human α-L-Fucosidase (h-Fuc) in pET22b(+). Vector pCMV.SPORT6 containing the human α-L-fucosidase gene served as a DNA template for PCR amplification. The upstream (5′-CTGCAGCACATATGGTGCGTCGGGCCCAGCCTC-3′) and downstream (5′-GGTACCGGATCCTCACTTCACTCCTGTCAGCT-3′) primers, containing *Nde*I and *Kpn*I restriction sites as underscored, respectively, were employed to amplify the *h-fuc* gene coding the mature protein. The first 22 amino acids in the intact gene constitute the signal peptide that was omitted from the DNA amplification. The amplified DNA fragment (∼1.4 kb) was subcloned into pET22b(+) for protein expression.

Site-Directed Mutagenesis in Vitro. The *h-fuc* gene was mutated with a kit (QuikChange; Stratagene) for site-directed mutagenesis. The primers to generate the mutations (underscored) were as follows: E70G(+), 5′-CCCGCCTGGGGCAGCGGCTGGTTCTGGTGGCAC-3′, and E70G(−), 5′-GTGCCACCAGAACCAGCCGCTGCCCCAGGCGGG-3′; E79G(+), 5′-GCACTGGCAGGGCGGGGGGCGGCCGCAG-3′, and E79G(−), 5′-CTGCGGCCGCCCCCCGCCCTGCCAGTGC-3′; E135G(+), 5′-ACGACAAAGCATCACGGCGGCTTCACAAAC-3′, and E135G(−), 5′-GTTTGTGAAGCCGCCGTGATGCTTTGTCGT-3′; D158G(+), 5′-TGGGGCCTCATCGGGGCTTGGTTCGTGAA-3′, and D158G(−), 5′-TTCACCAACCAAGCCCCGATGAGGCCCCA-3′; D225G(+), 5′-CTGATATGGTCTGGCGGGGAGTGGGAAT-3′, and D225N(−), 5′-ATTCCCACTCCCCGTTAGACCATATCAG-3′; D258G(+), 5′-GGTGGTAGTAAATGGCCGATGGGGTCAG-3′, and D258G(−), 5′- CTGACCCCATCGGCCATTTACTACCACC-3′; E275G(+), 5′-GGATACTATAACTGTGGAGATAAATTCAAGCC-3′, and E275G(−), 5′-GGCTTGAATTTATCCCTACAGTTATAGTATCC-3′; D276G(+), 5′-GATACTATAACTGTGAAGGCAAATTCAAGC-3′, and D276G(−), 5′-GCTTGAATTTGCCTTCACAGTTATAGTATC-3′; E289G(+), 5′-CAGATCACAAGTGGGGGATGTGCACCAG-3′, and E289Q(−), 5′-CTGGTGCACATCTGCCACTTGTGATCTG-3′. All mutations were confirmed with DNA sequencing. For those mutations for which significant enzyme activity was lost, the entire mutated genes were sequenced to confirm that only the intended mutations had occurred.

Expression and Purification of Recombinant Human α-L-Fucosidase Protein. E. coli BL21(DE3) cells bearing pET22_*h-fuc* plasmid were cultivated overnight in LB medium (50 mL, with 10 g of trypton, 5 g of yeast extract, and 5.5 g/L NaCl, pH 6.5, 37 °C). This culture (5 mL) was inoculated into the same medium (1 L) supplemented with ampicillin (final concentration 0.1 mg/mL). The expression of α-L-fucosidase was induced on addition of isopropyl thio-β-D-galactoside (1 mM, IPTG) for 8 h during which the OD_{600} value attained 2.4−2.6. Cells were harvested and then resuspended in sodium acetate buffer (20 mL, 20 mM, pH 5.5) for sonication. The crude proteins in the supernatant were precipitated on addition of ammonium sulfate to 85% saturation. The precipitant was resuspended in sodium acetate buffer (10 mL, 20 mM, pH 5.5). The solution was desalted on a column (HiTrap). The filtrate (15 mL) was loaded onto a cation-exchanged column (HiTrap SP, 2.6 × 40 cm) that was preequilibrated with sodium acetate buffer (20 mM, pH 5.5). Enzymes were eluted with acetate buffer and a linear gradient concentration of NaCl (0−1.0 M, 5 mM/min). The fractions with α-L-fucosidase activity (with NaCl at 450−550

Scheme 1: Preparation of Aryl α-L-Fucosides[a]

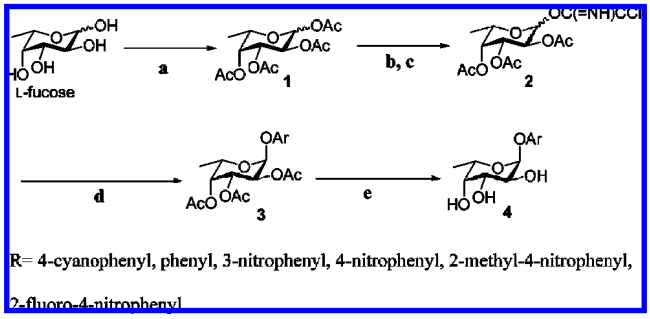

[a] Reagents and conditions: (a) Ac_2O, pyridine, ~25 °C, 8 h; (b) H_4N_2−HOAc, DMF, ~25 °C, 30 min; (c) Cl_3CCN, Cs_2CO_3, H_2CCl_2, ~25 °C, 8 h; (d) ROH (acceptor), TMSOT*f*, 4 Å MS, H_2CCl_2, −20 °C, 30 min; (e) NaOMe, MeOH, ~25 °C, 30 min.

mM) were collected, concentrated 25-fold, and preequilibrated with sodium phosphate buffer (20 mM, pH 6.2) for further chromatography. A sample (5 mL) was loaded onto an anion-exchange column (HiTrap Q, 1.6 × 20 cm) preequilibrated with sodium phosphate buffer (20 mM, pH 6.2). Proteins were eluted with a phosphate buffer and a linear gradient of concentration of NaCl (0−1.0 M, 6.5 mM/min). Fractions (200−300 mM NaCl) with activity were pooled (5 mL final) and concentrated 10-fold for further chromatography. A sample (1 mL) was loaded onto a column (Sephadex G-75, 1.6 × 20 cm) and eluted with sodium acetate buffer (20 mM, pH 5.5) containing NaCl (10 mM). Fractions with activity were collected and concentrated and kept at 4 °C for further tests. All purifications were performed at ambient temperature (~25 °C). To minimize enzyme cross-contamination during purification, a fresh column was used to purify each mutant. For the expression and purification of D225 and E289 mutants, the corresponding plasmids with a His_6 tag at the C-termini were constructed. A column (HiTrap HP, 1 × 5 cm) was used for purification of the protein in one step. The eluted protein was concentrated 15-fold and maintained at 4 °C for further tests. The concentration of the protein was determined according to the BCA (bicinchoninic acid) method, as described in the manufacturer's protocol (Sigma; BCA-1 kit), followed by measurement of absorption by the chromophore at 280 nm. The molecular mass of the purified enzyme was estimated with SDS−PAGE according to Laemmli (*44*).

Synthesis of the Substrate. 2-Chloro-4-nitrophenyl α-L-fucopyranoside (CNPF) was synthesized according to a published method (*45*). All other aryl α-L-fucopyranosides including phenyl α-L-fucopyranoside (PF), *p*-cyanophenyl α-L-fucopyranoside (pCPF), *m*-nitrophenyl α-L-fucopyranoside (mNPF), *p*-nitrophenyl α-L-fucopyranoside (pNPF), 2-methyl-4-nitrophenyl α-L-fucopyranoside (MeNPF), and 2-fluoro-4-nitrophenyl α-L-fucopyranoside (FNPF) were synthesized according to our protocol as outlined in Scheme 1. The synthesis began with the selective removal of the anomeric acetyl group in peracetylated α-L-fucopyranosides **1** with hydrazine acetate (*46*). Subsequent treatment of the resulting hemiacetal with excess of trichloroacetonitrile in large excess and in the presence of Cs_2CO_3 (8 h, ~25 °C) (*47*) produced the thermodynamically stable 2,3,4-tri-*O*-acetyl-L-fucopyranosyl 2,2,2-trichloroacetimidate (TAF) **2** (*48*). TAF was then coupled with various phenols in the presence of TMSOTf to afford the corresponding peracetylated aryl α-L-fucopyranosides **3** as the single anomer. After deprotection with NaOMe, aryl α-L-fucopyranosides **4** were obtained. Detailed procedures will be published elsewhere. All substrates were purified with column chromatography; their structures were confirmed with NMR spectra, which yielded the following data.

FNPF, ^{1}H NMR (300 MHz, CD_3OD) δ/ppm: 1.07 (d, J = 6.5 Hz, 3H, H-6), 3.81 (m, H-4, 2H, H-5), 3.94 (dd, J = 3.5, 9.6 Hz, 1H, H-3), 4.08 (dd, J = 7.3, 9.6 Hz, 1H, H-2), 5.77 (d, J = 3.16 Hz, 1H, H-1), 7.37 (d, J = 9.2 Hz, 1H, ArH), 8.06 (dd, J = 2.6, 9.2 Hz, 1H, ArH), 8.85 (d, J = 2.6 Hz, 1H, ArH). CNPF, ^{1}H NMR (300 MHz, CD_3OD) δ/ppm: 1.13 (d, J = 6.6 Hz, 3H, H-6), 3.74−3.83 (m, 2H, H-4, H-5), 3.95 (dd, J = 3.6, 9.6 Hz, 1H, H-3), 4.33 (dd, J = 7.6, 9.6 Hz, 1H, H-2), 5.71 (d, J = 3.78 Hz, 1H, H-1), 7.31 (d, J = 9.2 Hz, 1H, ArH), 8.08 (dd, J = 2.6, 9.2 Hz, 1H, ArH), 8.85(d, J = 2.6 Hz, 1H, ArH). pNPF, ^{1}H NMR (300 MHz, CD_3OD) δ/ppm: 1.22 (d, J = 6.0 Hz, 3H, H-6), 3.72−3.8 (m, 2H, H-4, H-5), 3.94 (dd, J = 3.0, 9.0 Hz, 1H, H-3), 4.30 (dd, J = 7.2, 9.1 Hz, 1H, H-2), 5.87 (d, J = 4.0 Hz, 1H, H-1), 7.33 (d, J = 8.7 Hz, 2H, ArH), 8.32 (d, J = 9.3 Hz, 2H, ArH). MeNPF, ^{1}H NMR (300 MHz, CD_3OD) δ/ppm: 1.20 (d, J = 6.4 Hz, 3H, H-6), 2.37 (s, 3H, CH_3), 3.72−3.78 (m, 2H, H-4, H-5), 3.96 (dd, J = 3.6, 9.6 Hz, 1H, H-3), 4.02 (dd, J = 7.6, 9.6 Hz, 1H, H-2), 5.70 (d, J = 4.88 Hz, 1H, H-1), 7.28 (d, J = 9.8 Hz, 1H, ArH), 8.08 (dd, J = 2.6, 9.6 Hz, 1H, ArH), 8.11 (d, J = 2.6 Hz, 1H, ArH). mNPF, ^{1}H NMR (300 MHz, CD_3OD) δ/ppm: 1.25 (d, J = 7.0 Hz, 3H, H-6), 3.66−3.72 (m, 2H, H-4, H-5), 3.8 (dd, J = 3.5, 9.6 Hz, 1H, H-3), 4.16 (dd, J = 6.9, 9.3 Hz, 1H, H-2), 5.73 (d, J = 3.6 Hz, 1H, H-1), 7.41−7.37 (m, 1H, ArH), 7.50−7.45 (m, 1H, ArH), 7.94−7.90 (m, 2H, ArH). pCPF, ^{1}H NMR (300 MHz, CD_3OD) δ/ppm: 1.21 (d, J = 6.8 Hz, 3H, H-6), 3.7−3.76 (m, 2H, H-4, H-5), 3.87 (dd, J = 3.0, 9.0 Hz, 1H, H-3), 4.16 (dd, J = 7.2, 9.1 Hz, 1H, H-2), 5.83 (d, J = 3.6 Hz, 1H, H-1), 7.12 (d, J = 8.7 Hz, 2H, ArH), 7.65 (d, J = 8.9 Hz, 2H, ArH). PF, ^{1}H NMR (300 MHz, CD_3OD) δ/ppm: 1.25 (d, J = 7.0 Hz, 3H, H-6), 3.74−3.82 (m, 2H, H-4, H-5), 3.97 (dd, J = 3.6, 9.0 Hz, 1H, H-3), 4.3 (dd, J = 7.2, 9.5 Hz, 1H, H-2), 5.74 (d, J = 3.6 Hz, 1H, H-1), 7.07−6.81 (m, 3H, ArH), 7.33−7.21 (t, 2H, ArH).

Kinetic Experiments. Enzymatic activity was determined in sodium acetate buffer (50 mM, pH 5.0, 37 °C) on monitoring the hydrolysis of *p*-nitrophenyl α-L-fucopyranoside (pNPF, 0.5 mM) to release *p*-nitrophenol (or *p*-nitrophenolate). Reactions were monitored at the isosbestic point (348 nm) of *p*-nitrophenol and *p*-nitrophenolate with a spectrophotometer (Hewlett-Packard 8453) equipped with a circulating water bath at 37 °C. One unit of enzyme is defined as the amount required to release *p*-nitrophenol (1 μmol for 1 min) from the substrate. For kinetic experiments, all reactions were performed in sodium phosphate buffer (50 mM, pH 6.8, 37 °C). The Michaelis parameter was evaluated for each synthetic substrate with nonlinear regression analysis (EnzFitter program) (*49*). Reaction rates were determined (in triplicate, pH 6.8, 37 °C) with each of six substrates at a concentration in a range 0.1−1 mM for wild-type enzyme and 0.03−1 mM for E289G. The wavelengths employed and molar absorption coefficients (M^{-1} cm^{-1}) at those wavelengths for each substrate are CNPF, ϵ(420 nm) = 3038;

FNPF, ϵ(400 nm) = 2806; pNPF, ϵ(400 nm) = 7280; MeNPF, ϵ(400 nm) = 6300; mNPF, ϵ(380 nm) = 385; pCPF, ϵ(270 nm) = 3101; PF, ϵ(277 nm) = 228.

Activation of h-Fuc Mutants with Azide. The rates of hydrolysis of CNPF, FNPF, and pNPF by E289G in the presence of azide (0−2 M) were examined with a substrate (0.1−1.0 mM) in phosphate buffer (50 mM, pH 6.8, 37 °C). The absorption coefficients of the corresponding phenols at pH 6.8 are listed above. At the tested conditions, the reaction was linear during the first 5 min of incubation. All kinetic data are calculated as the mean of at least two experiments and were further fitted with nonlinear regression analysis (*49*).

^{1}H Nuclear Magnetic Resonance (NMR) Analysis of the Rescue Product. The hydrolysis of CNPF by E289G in the presence of sodium azide was monitored with NMR spectra (samples at 30 °C). To monitor the chemical rescue by NMR, we prepared the E289G mutant, CNPF, and sodium azide in a deuterated phosphate buffer (5 mM, pH 6.8). After the spectrum of CNPF was recorded, the reaction was initiated on adding E289G and sodium azide (final concentrations 1.4 mg/mL and 1.5 M, respectively); the final concentration of CNPF was 7.5 mM. ^{1}H NMR spectra were recorded as a function of time.

The chemical rescue reaction catalyzed with D225G was performed with sodium azide (1.5 M) and substrate FNPF (64 mM) in phosphate buffer (50 mM, pH 6.5, 37 °C). The reaction mixture containing product β-fucosyl azide was collected and concentrated. Acetylation of the concentrated mixture with acetic anhydride was conducted overnight (~25 °C). The peracetylated β-fucosyl azides were further purified on a chromatographic column and analyzed with ^{1}H NMR spectra (solvent $DCCl_3$; its signal served as internal reference standard). ^{1}H NMR signals are assigned as follows: 4.58 (d, J = 8.5 Hz, 1H, H-1), 5.03 (dd, J = 3.3 Hz, 1H, H-3), 5.13 (dd, J = 1.7, 8.6 Hz, 1H, H-2), 5.25 (d, J = 4.3 Hz, 1H, H-4), 3.91 (q, J = 5.4, 13.0 Hz, 1H, H-5), 1.23 (d, J = 6.4 Hz, 3H, H-6).

Mass Spectral Analysis. With a quadrupole time-of-flight mass filter we scanned the mass spectrum with a ratio m/z of mass to charge in a range 100−2500 units, scan speed 2 s per step, and interscan duration 0.1 s per step. In all ESI-MS experiments, the quadrupole scan mode was applied (capillary needle at 3 kV, source block temperature 80 °C, desolvation temperature 150 °C). The mass of proteins in their desalted forms used for these measurements was normally within a range 5−10 μg.

CD Spectra of Recombinant Human α-L-Fucosidase. Spectra were measured with a spectropolarimeter (JASCO J-815, cell length 1 mm, 25 °C) from 200 to 300 nm and corrected for the buffer background; 16 spectra were recorded and averaged. The concentration of proteins used for CD measurement was 1 mg/mL.

RESULTS AND DISCUSSION

Structure Modeling and Multiple Sequence Alignment. With the available structure and function information, Tm-Fuc, the closest bacterial relative mammalian counterpart, served as a template to identify the candidates for catalytically essential residues of h-Fuc (*42*). Tm-Fuc is a two-domain protein: the N-terminal domain (7−359) adopts a TIM-barrel-like fold and the C-terminal (360−447) domain adopts a β-sandwich-like fold (*42*). Instead of eight helices, the eight parallel β-strands in the barrel center are surrounded by six helices. α5 and α6 were missing or could not be modeled. Nucleophile D224 and catalytic acid/base E266 are located at the ends of β4 and β6, respectively. Because the catalytic pocket of Tm-Fuc is located at the TIM-barrel domain, the h-Fuc 3D structure prediction and multiple sequence alignment were performed for the segments of the TIM-barrel domain only. Except regions 45−64 and 177−188 (numbered according to Tm-Fuc), the Swiss-modeled structure of h-Fuc (data not shown) is similar to the structure of Tm-Fuc (PDB 1hl8) (rmsd = 0.8 Å; Z-score = 7.3). It was thus adequate to use Tm-Fuc as a template.

A set of h-Fuc close homologues was aligned using Praline, a multiple sequence alignment method that takes predicted secondary structure information into account during alignment. Multiple methods (including T-Coffee, ClustalW, and MUSCLE) of sequence alignment were also used to align these sequences, and similar alignments were obtained. The results derived from Praline alignment and the functionally important information of Tm-Fuc (*42*) are shown in Figure 2. As the alignment indicates, the residues of the nucleophile (D224 of Tm-Fuc) and nearby residues are highly conserved whereas the conservation of catalytic acid/base and nearby residues is much less evident. Except residues in the region of Tm-Fuc 45−64, most residues playing an important role in the interaction between Tm-Fuc and fucose are also conserved within the h-Fuc close homologues. On the basis of their sharing similar sequence/structure and their conservation of a catalytic pocket and nucleophile, it was possible to select rationally the candidates of the general acid/base residue. Including D225, in total 13 positions with conserved D, E, and mixed D and E, shown in Figure 2, might be structurally or functionally important. According to a general catalytic property of TIM barrel proteins, the catalytic important residues are commonly located near the ends of the β-strand of the TIM barrel. Conserved residues that are remote from these locations are thus less likely to be catalytically important residues. The distance between the carboxyl groups of nucleophile and catalytic acid/base residues is typically about 6 Å. As no experimentally determined 3D structure of h-Fuc was available, the average Cα−Cα distance ($d_{C\alpha-C\alpha}$) between Tm-Fuc D224 and the equivalent D/E served to evaluate the candidacy of a catalytic acid/base. The truncation distance was set at 20 Å. According to the proximity to the end of the β-strand and $d_{C\alpha-C\alpha}$, three conserved residues, D225, D258, and E289 in h-Fuc, were identified as candidates. E275 and D276, which are possible equivalents of Tm-Fuc E266 although the homology is not evident, are also suggested.

Expression, Purification, and Characterization of Recombinant h-Fuc. The *h-fuc* gene encoding the mature protein of human α-L-fucosidase (h-Fuc) was subcloned into pET22b(+). The resulting plasmid was transformed into the *E. coli* BL21(DE3) strain and cultivated in LB medium (37 °C, pH 6.5). The recombinant enzyme, expressed as a soluble form, was further isolated to become highly homogeneous with purification in several consecutive steps, including precipitation with ammonium sulfate and use of chromatographic columns in a series. The final yield was 5%; 33-fold purification was achieved. The purity of the recombinant

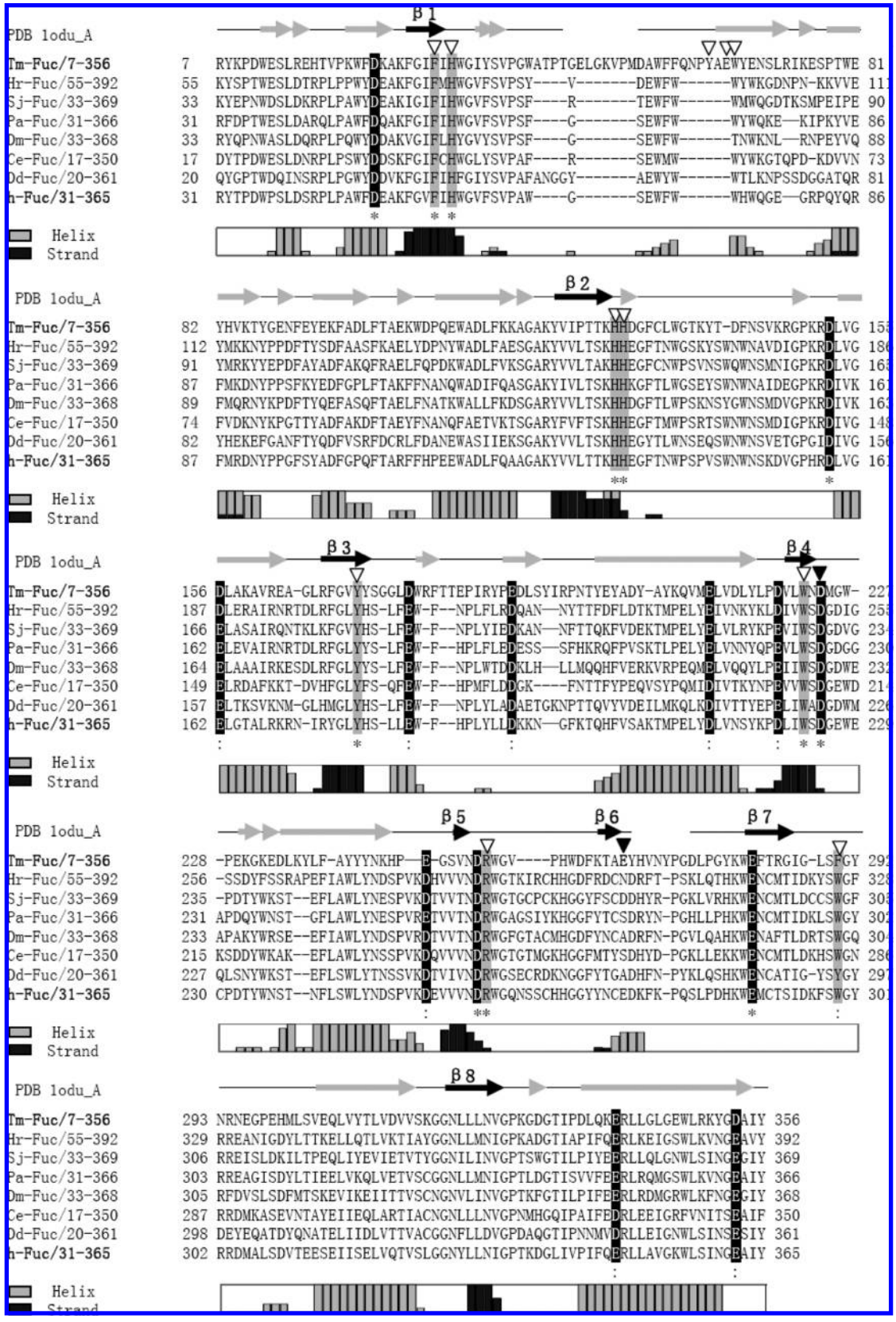

FIGURE 2: Multiple sequence alignment of the TIM barrel domain of *T. maritima* and human α-L-fucosidase close homologues. Secondary structure elements (SSE) of Tm-Fuc based on PDB 1odu are shown at the top of the alignment, and the propensity of PSI-Pred SSE of close homologues of h-Fuc is expressed at the bottom. Catalytic nucleophile and general acid/base of Tm-Fuc are denoted ▼, and the residues that interact with fucose within the catalytic pocket (1odu) are denoted ▽. The columns containing D and E only are shown in black; the columns with positional homology to the Tm-Fuc catalytic pocket are shown in gray. These columns are labeled with ★ if the equivalent residues are identical or with : if they are similar. The UniProt accession numbers of the studied fucosidases follow: *T. maritima* Q9WYE2 (Tm-Fuc), *H. roretzi* Q8TA71 (Hr-Fuc), *S. japonicum* Q86FH9 (Sj-Fuc), *P. abelii* Q5RFI5 (Pa-Fuc), *D. melanogaster* Q9VTJ4 (Dm-Fuc), *C. elegans* P49713 (Ce-Fuc), and *D. discoideum* P10901 (Dd-Fuc). As the tested h-Fuc differs slightly from the corresponding UniProt P04066, the position of a residue is specified according to NCBI M29877.

h-Fuc (homogeneity >95%) was analyzed with SDS−PAGE, and its molecular mass was confirmed with ESI/MS (data not shown). Although the expression of h-Fuc in *E. coli* was reported by de Carlos et al. (*33*), the recombinant protein was an insoluble glutathione *S*-transferase fusion protein. Cultivation of the culture with LB medium (pH 6.0−6.5) is a crucial condition to maintain the recombinant h-Fuc in active form. A greater pH (≥7.0) yielded a soluble but only inactive enzyme. The recombinant h-Fuc was stable up to 55 °C with incubation (4 h, pH 7.0); the optimum temperature for h-Fuc is approximately 55 °C. The stability of the enzyme to pH was investigated with pNPF as the substrate. In general, the enzyme was stable at pH 2.5−8.0 for 4 h; the enzyme activity decreased greatly for pH greater than 8.0 or less than 2.0. An assay of pH-dependent activity showed that the recombinant enzyme had optimum activity at pH 4.8−5.2 (data not shown). The features exhibited above are comparable with the native human liver enzyme, but the activity differs somewhat. For instance, at pH 5.0, the catalytic activity of recombinant h-Fuc (K_m = 0.105 mM, k_{cat} = 48.6 s^{-1}) with pNPF as substrate was 12 times that of a counterpart purified from human liver tissue (K_m = 0.43 mM, k_{cat} =16.3 s^{-1}) (*29, 50*).

Mutagenic Study of h-Fuc. The first solved protein structure of α-L-fucosidase was from *T. maritima* (Tm-Fuc) (*42*). This structure provides valuable information as a basis for speculation about the catalytic mechanism and essential residues of the enzyme. Tm-Fuc possesses identity ~38% with h-Fuc and thus allows a reliable modeling of h-Fuc based on the crystal structure of Tm-Fuc. Comparison of these structures showed that large differences are present at the periphery of the catalytic site, which might result in an enlarged access to the catalytic site of h-Fuc, and for which a distinct substrate binding was suggested (*42*).

Based on both structural information for a Tm-Fuc−product complex and for a covalent glycosyl-enzyme intermediate and kinetic and mutagenesis experiments, Asp^{224} and Glu^{266} of Tm-Fuc were identified to function as the catalytic nucleophile and the acid/base catalyst, respectively. As almost all known retaining α-L-fucosidases are grouped in GH-29, this Tm-Fuc structure is prospectively valuable to unwind the catalytic function of an enzyme in this family, including human α-L-fucosidase (h-Fuc). Extensive amino acid alignment of various α-L-fucosidases reveals that the catalytic nucleophile is highly conserved whereas the acid/base catalyst had no reliable consistency. Asp^{225} (Asp^{224} in Tm-Fuc) seems to serve as the nucleophile in h-Fuc, but the residue that functions as the general acid/base catalyst is obscure. Nine residues in h-Fuc, Glu^{70}, Glu^{79}, Glu^{135}, Asp^{158}, Asp^{225}, Asp^{258}, Glu^{275}, Asp^{276}, and Glu^{289}, having a carboxylic acid side chain and derived from structure modeling and multiple sequence alignment (as described in a preceding section), were chosen for mutagenic tests. All potential aspartates and glutamates were converted into asparagine, glutamine, or glycine through site-directed mutagenesis. The kinetic parameters of h-Fuc and its mutants are summarized in Table 1. Values of k_{cat} and K_m of the mutants were insignificantly influenced, other than those mutations at Asp^{225} and Glu^{289}. The secondary structures of wild-type h-Fuc and its mutants, such as D225G, D276N, and E289G, were analyzed according to their CD spectra; the results indicate that no significant perturbation of the structure occurred (Figure 3). When pNPF served as substrate, the activity (k_{cat}/K_m) of D225N and D225G was about 1/21000 that of the wild-type enzyme, whereas K_m values increased only 3.7-fold, indicating Asp^{225} to be the catalytic nucleophile of h-Fuc. This prediction is consistent with the test on bacterial α-L-fucosidases (*38, 39*). Further evidence to support this conclusion is presented in a succeeding section. The hydrolysis of pNPF catalyzed with E289Q (or E289G) yielded 428-fold (342-fold), 2.5-fold (2.3-fold), and 168-fold (146-fold) decreases of k_{cat}, K_m, and k_{cat}/K_m, respectively. The small value of K_m, likely indicating an accumulation of fucosyl-enzyme intermediate (*51*), and the loss of activity of mutants might imply an important role played by Glu^{289}.

Table 1: Kinetic Parameters of pNPF Catalyzed with Wild-Type and Mutant h-Fuc[a]

enzyme	k_{cat}/s^{-1}	$^{r}k_{cat}/\%$	K_m/mM	$k_{cat}/K_m/M^{-1}$ s^{-1}	$^{r}k_{cat}/K_m/\%$
wild type	17.1 ± 0.3	100	0.28 ± 0.02	61070	100
E70G	16.9 ± 0.2	99	0.28 ± 0.01	60360	99
E79G	16.3 ± 0.2	95	0.30 ± 0.01	54330	89
E135G	16.0 ± 0.3	93	0.28 ± 0.03	57140	94
D158G	16.9 ± 0.1	99	0.28 ± 0.01	60360	99
D258G	13.5 ± 0.2	79	0.27 ± 0.02	49485	81
E275G	16.9 ± 0.1	99	0.28 ± 0.02	60360	99
D276G	16.7 ± 0.2	97	0.28 ± 0.01	59290	97
D225G	0.003 ± 0.001	0.017	1.04 ± 0.06	2.9	0.0047
D225N	0.003 ± 0.001	0.017	1.06 ± 0.04	2.8	0.0046
E289Q	0.039 ± 0.005	0.23	0.11 ± 0.02	364	0.60
E289G	0.048 ± 0.004	0.28	0.12 ± 0.02	417	0.68

[a] Assays were performed in sodium phosphate buffer (50 mM, pH 6.8, 37 °C).

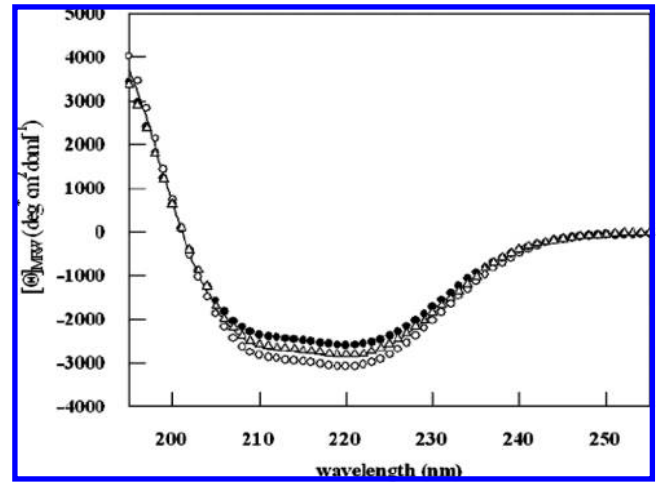

FIGURE 3: CD spectra of human α-L-fucosidase and its mutants. Mutants of D225G (○), E289G (●), and D276G (□) exhibit CD spectra similar to that of the wild-type enzyme (solid line).

Substrate Reactivity. With broad specificity of the aglycon moiety, to determine the kinetic parameters of the enzyme for hydrolysis of various aryl substrates bearing leaving groups with varied pK_a is a common strategy in an investigation of the mechanistic action of glycoside hydrolase (*51, 52*). The catalysis of a GH family with a two-step, double displacement mechanism typically involves formation of a glycosyl-enzyme intermediate on glycosylation followed by deglycosylation on decomposition of the intermediate. The aglycon moiety is cleaved during glycosylation in the reaction (Figure 1). The rate of reaction of this glycosylation is dictated by the leaving group ability of the aglycon. A reasonable correlation between the pK_a of the phenol and

Table 2: Kinetic Parameters of Aryl α-L-Fucosides Catalyzed with Wild-Type h-Fuc and E289G[a]

		k_{cat}/s^{-1}		K_m/mM		$k_{cat}/K_m/s^{-1}$ M^{-1}		$\log(k_{cat})/s^{-1}$		$\log(k_{cat}/K_m)/s^{-1}$ M^{-1}	
substrate	pK_a	WT	E289G	WT	E289G	WT	E289G	WT	E289G	WT	E289G
CNPF	5.42	18.8 ± 0.2	0.14 ± 0.02	0.27 ± 0.02	0.052 ± 0.007	69630	2800	1.27	−0.85	4.84	3.45
FNPF	6.20	18.2 ± 0.3	0.12 ± 0.02	0.28 ± 0.02	0.078 ± 0.009	65000	1500	1.26	−0.92	4.81	3.18
pNPF	7.18	17.1 ± 0.3	0.05 ± 0.01	0.28 ± 0.02	0.12 ± 0.01	61070	416	1.23	−1.30	4.78	2.62
MeNPF	7.42	13.6 ± 0.4	0.012 ± 0.002	0.48 ± 0.03	0.21 ± 0.02	28330	50	1.13	−2.00	4.45	1.70
mNPF	8.39	9.0 ± 0.6	0.0032 ± 0.0005	0.34 ± 0.04	0.17 ± 0.01	26470	21	0.95	−2.52	4.42	1.32
pCPF	8.49	8.9 ± 0.5	0.0022 ± 0.0005	0.71 ± 0.05	0.33 ± 0.03	12535	6	0.95	−2.70	4.1	0.78
PF	9.99	5.5 ± 0.9	0.0001 ± 0.00003	1.18 ± 0.11	0.41 ± 0.04	4240	0.2	0.74	−4.00	3.63	−0.70

[a] Enzymatic assays were performed in sodium phosphate buffer (50 mM, pH 6.8, 37 °C).

rate parameters dominated by the glycosylation step is expected: this correlation is expected to be observed at all pK_a values of the leaving group for k_{cat}/K_m. If glycosylation completely determines k_{cat}, β_{lg} similar to that for k_{cat}/K_m should be obtained, whereas if deglycosylation completely determines k_{cat}, this parameter should be independent of the substrate. Because the substrate synthesis is complicated, the substrate reactivity of α-L-fucosidase, including bacterial and mammalian enzymes, has never been investigated. We developed a facile protocol to prepare chromophoric substrates, which allows us to characterize the catalysis of h-Fuc in detail. The rate-limiting step of hydrolysis catalyzed by the recombinant h-Fuc was solved on using aryl α-L-fucopyranosides with varied leaving phenols (pK_a values 5.42−9.99). The kinetic parameters of the enzymatic reaction toward substrates are summarized in Table 2. Little variation of the K_m values (0.27−1.18 mM) and k_{cat} (5.5−18.8 s^{-1}) was observed. From calculations with these data we constructed the Brønsted relation, which is useful for an understanding of the mechanism of enzyme action (*52*−*56*). Based on k_{cat} values, an extended Brønsted plot was established on plotting the logarithm of k_{cat} against pK_a of the leaving phenol (Figure 4a). A plot with a slightly downward trend was obtained, with a slope −0.13 signifying the value of Brønsted parameter β_{lg}. As k_{cat} values of the tested substrates vary over a factor of 3, the small magnitude of β_{lg} (derived from k_{cat}) might indicate that fucosylation is the rate-limiting step, involving a substantial proton transfer from the general acid residue to the oxygen of the leaving phenol. However, to further confirm this viewpoint, more experiments such as secondary kinetic isotope effect and nucleophilic competition will need to be performed.

To verify the catalytic role of Glu^{289}, we employed the E289G mutant also for an assay of substrate reactivity; we obtained a biphasic Brønsted plot (Figure 4a). The catalytic activity of E289G toward a poor substrate (with a leaving phenol of pK_a > 7) correlated well with the pK_a of the leaving phenol with $\beta_{lg} = -0.88$, indicating that the formation of a fucosyl-enzyme intermediate (in the fucosylation step) became the rate-limiting step, whereas values of k_{cat} for activated substrates (with a leaving phenol of pK_a < 7) were almost constant, indicating that defucosylation is rate-limiting when activated substrates are hydrolyzed. In principle, the hydrolysis of poor substrates, such as pCPF and PF, requires assistance of a strong acid from the general acid/base catalyst in the fucosylation step. The rate of fucosylation is much smaller than for activated substrates, such as CNPF and FNPF, which require less assistance from a general acid/base residue. The variation of the rate-limiting step on E289G catalysis toward a poor substrate is attributed to an absence

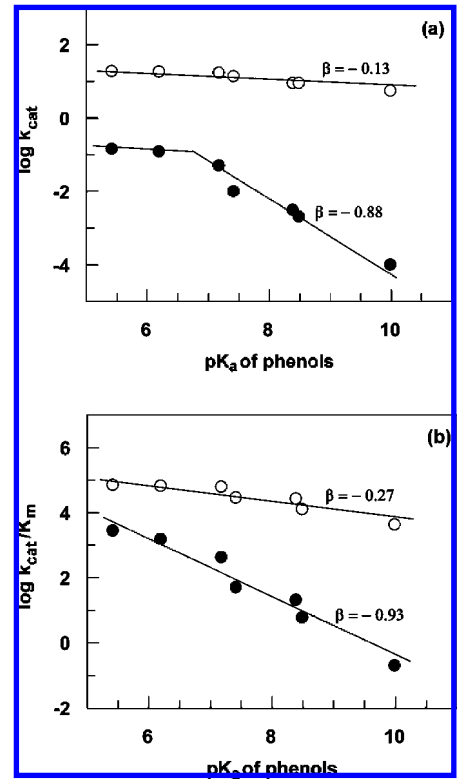

FIGURE 4: Brønsted plots of wild-type α-L-fucosidase (○) and E289G (●). Plots of $\log(k_{cat})$ (a) and $\log(k_{cat}/K_m)$ (b) against pK_a of the leaving phenol.

of a general acid/base residue. The hydrolysis of CNPF and FNPF (activated substrates) catalyzed with E289G exhibited K_m values 0.05 and 0.08 mM, respectively, smaller than that of the wild-type enzyme, K_m = 0.28 mM, reflecting an accumulation of the fucosyl-enzyme intermediate during the enzymatic reaction. This condition is appreciated if one notes that K_m can be represented as $[E][S]/\sum[ES]$; the greater the accumulation of the fucosyl-enzyme intermediate, the smaller is thus the K_m value. For an activated substrate the rate of fucosylation is much increased with an effective leaving phenol (relative to that of a poor substrate) with less assistance from the general acid/base catalyst, whereas the second step remains slow as the basic residue, expected to activate the water molecule for catalysis in the wild-type enzyme, is then lacking. The second-order coefficient k_{cat}/K_m for the rate is composed of rate coefficients along the reaction pathway from the free enzyme to the first chemical step (i.e., fucosylation). It is thus useful to probe the fucosylation with respect to the degree of bond cleavage via the Brønsted constant, which is the slope of an extended Brønsted plot: $\log(k_{cat}/K_m)$ vs pK_a of the phenols. A plot

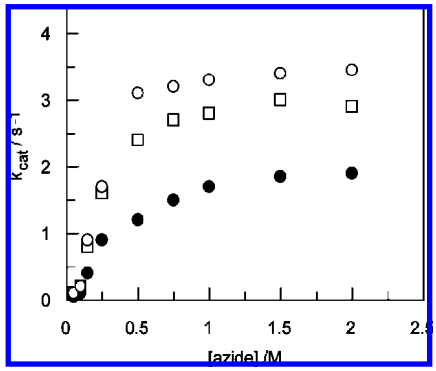

FIGURE 5: Plot of k_{cat} vs concentration of sodium azide for aryl fucosides catalyzed with E289G: CNPF (○), FNPF (□), and pNPF (●).

(Figure 4b) reveals a Brønsted parameter of value $\beta_{lg} = -0.27$ for the catalysis of the wild-type enzyme. This small magnitude of β_{lg} indicates that a little negative charge developed on the oxygen atom of the leaving phenol, resulting from proton donation by the acid/base catalyst; no proton donation would have occurred when the general acid/base residue was removed in the E289G mutant. The catalytic efficiency (k_{cat}/K_m) for the tested substrates tends consequently to be highly sensitive to the leaving ability of a phenol group. A much larger magnitude of the Brønsted parameter, $\beta_{lg} = -0.93$ (Figure 4b), was thus observed in the catalysis of E289G.

Rate Enhancement by Azide. As shown above, the rate-limiting step of the wild-type h-Fuc-catalyzed hydrolysis of the tested substrates (pK_a of leaving phenols 5.42−9.99) is defucosylation (Figure 1). Except for an activated substrate (e.g., CNPF and FNPF) that scarcely requires assistance from a general acid, the lack of the acid/base catalyst makes the fucosidic bond in a poor substrate difficult to hydrolyze and consequently alters the rate-limiting step of the reaction to fucosylation (Figure 4a). For an activated substrate, removal of the acid/base catalyst results in defucosylation becoming even more rate-limiting. An accumulation of the fucosyl-enzyme intermediate consequently becomes observable and is reflected in a decreased K_m value. Two other strategies commonly applied to investigate the presence of a glycosyl-enzyme intermediate are direct measurement of the molecular mass of the protein by mass spectrometry (discussed in a later section) and chemical rescue with small nucleophiles.

Chemical rescue of the activities of D225G and E289G was employed to elucidate the functions for both residues. Replacing the essential groups with a small glycine residue presumably results in space in the active site sufficient that a small nucleophile becomes accommodated in this cavity near the α-face of the substrate (in the case of E289G) or the β-face of the fucosyl-enzyme intermediate (in the case of D225G). The activities of such mutated enzymes might be partially recovered if the small ion functions as a nucleophile or a general base. Enhancement of the rate on adding an external nucleophile was observed in some α-fucosidases, such as Ss-Fuc (*57*) and Tm-Fuc (*39*), and many other glycoside hydrolases (*58, 59*). We employed sodium azide to reactivate D225G and E289G. A preliminary test using pNPF (1 mM) as the substrate showed that, in the presence of sodium azide (1 M), the activities of E289G and D225G were enhanced 30-fold and 6-fold, respectively, whereas the wild-type enzyme exhibited no significant variation. We used azide for extensive rescue tests also on E289G with CNPF, FNPF, and pNPF as substrate. In the presence of azide, the plateau in the increase of k_{cat} for the hydrolysis of activated substrates with E289G and azide at a large concentration (Figure 5) cannot be due to saturation of a binding site for azide because the final rates vary

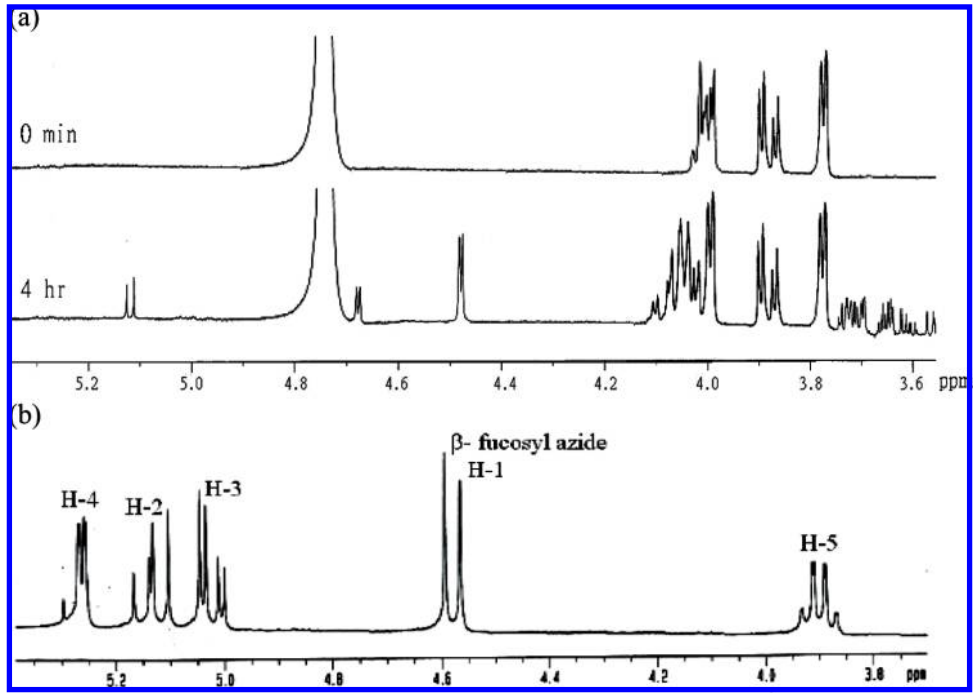

FIGURE 6: ^{1}H NMR spectral analysis of enzymatic products derived from azide rescue. (a) The reaction was catalyzed with E289G; the reaction mixture was employed directly for NMR spectral measurement with these assignments: C1-H of α-fucose, 4.48 (d, $J = 3.9$ Hz); C1-H of β-fucose, 5.12 (d, $J = 8.1$ Hz); C1-H of α-fucosyl azide, 4.68 (d, $J = 4.2$ Hz). (b) The reaction was catalyzed with D225G. The peracetylated β-fucosyl azide was isolated and analyzed with the assignments shown on the spectrum. The typical C1-H is at 4.58 ppm (d, $J = 8.5$ Hz).

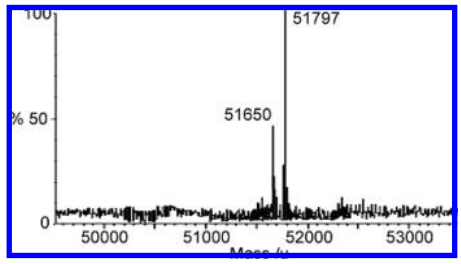

FIGURE 7: Apparent molecular mass of the E289G mutant after incubation with pNPF (8.5 mM) overnight. The signal corresponding to molecular mass 51650 units pertains to the unlabeled E289G mutant. The signal corresponding to molecular mass 51797 units, 147 units greater than that of E289G, pertains to an enzyme labeled with a fucosyl residue. E289G was constructed with a His_6 tag at the C-terminus of the polypeptide chain. The molecular mass of the His_6 tag E289G is calculated to be 51648 units.

markedly for each substrate. The curvature is likely due to another rate-determining step: with increasing concentration of azide, the rate of defucosylation increases, until fucosylation becomes rate-determining. The final rate observed (plateau value) correlates with the leaving group ability of the phenol, as would be expected if fucosylation becomes rate-limiting at the increased azide concentration.

This rate enhancement implies that azide ion might function as a nucleophile or a general base to activate the catalysis of the mutants. When azide serves as a nucleophile, a glycosyl azide might be produced. On the basis of the configuration of the glycosyl azide derived from the catalytic reaction of the mutant, one can determine the function of the essential residue. The anomeric configuration of the glycosyl azide is retained in the case of catalysis conducted by the mutant at a general acid/base residue, whereas the nucleophile mutant might yield the inverted ones (*56*). The temporal course of a NMR spectral experiment for an azide rescue on E289G catalysis showed that both α-fucosyl azide (doublet at 4.68 ppm, $J = 4.2$ Hz, corresponding to the C1 proton of the α-anomer) and fucose (for the β-pyranose, 5.12 ppm, $J = 8.1$ Hz; for the α-pyranose, 4.48 ppm, $J = 3.9$ Hz) were formed during the reaction (Figure 6a). Based on assignment of signals and integration of the signal for the C1 proton on the sugar ring, the ratio fucosyl azide/fucose was 0.18. The detection of α-fucosyl azide produced from E289G catalysis confirms that Glu^{289} is the general acid/base catalyst of h-Fuc. The peracetylated β-fucosyl azide, derived from a direct acetylation of the reaction product catalyzed with D225G and having a typical doublet at 4.58 ppm ($J = 8.5$ Hz, corresponding to the C1 proton of the β-anomer) (*38*), was detected on reactivation of the D225G catalysis (Figure 6b). The fucosyl azide produced by the D225G mutant was found to have a configuration inverted relative to the substrate, leading us to conclude that Asp^{225} is the catalytic nucleophile of h-Fuc.

Direct Evidence of Glu^{289} as the Acid/Base Catalyst. The main function of the general acid/base catalyst is to polarize a water molecule, especially for an activated substrate, thereby enhancing the nucleophilicity of the water molecule when it attacks the putative fucosyl-enzyme intermediate. Removing the acid/base catalyst likely produces an accumulation of the intermediate. This expectation is supported by an observation of a small K_m value, 0.063 mM, for CNPF with E289G. An ESI-MS measurement provided direct and conclusive evidence for this condition. As Figure 7 shows, a major protein signal corresponding to a molar mass 51797 Da was newly observed after incubation overnight of E289G with pNPF. The observation of an expected increase 147 units in molar mass, which was absent in the control experiment using wild-type h-Fuc, confirmed that a fucosyl residue became covalently labeled on the enzyme. This result clearly provides the first strong evidence that Glu^{289} is the general acid/base catalyst of human α-L-fucosidase. Although h-Fuc and Tm-Fuc possess substantial identity of amino acid sequences, the corresponding residues functioning as the general acid/base catalyst in both enzymes are inconsistent. Drawing further deductions about this discrepancy is difficult because the identification of E266 as the general acid/base catalyst in Tm-Fuc was strongly supported by the crystal structure of a covalent fucosyl-enzyme intermediate and the kinetic investigation of the E266A mutant (*42*).

REFERENCES

1. Moloney, D. J., Shair, L. H., Lu, F. M., Xia, J., Locke, R., Matta, K. L., and Haltiwanger, R. S. (2000) Mammalian Notch1 is modified with two unusual forms of *O*-linked glycosylation found on epidermal growth factor-like modules. *J. Biol. Chem. 275*, 9604–9611.
2. Ayude, D., Fernandez-Rodriguez, J., Rodriguez-Berrocal, F. J., Martinez-Zorzano, V. S., de Carlos, A., Gil, E., and de la Cadena, M. P. (2000) Value of the serum α-L-fucosidase activity in the diagnosis of colorectal cancer. *Oncology 59*, 310–316.
3. Hiraishi, K., Suzuki, K., Hakomori, S., and Adachi, M. (1993) Le^y antigen expression is correlated with apoptosis (programmed cell death). *Glycobiology 3*, 381–390.
4. Becker, D. J., and Lowe, J. B. (1999) Leukocyte adhesion deficiency type II. *Biochim. Biophys. Acta 1455*, 193–204.
5. Becker, D. J., and Lowe, J. B. (2003) Fucose: biosynthesis and biological function in mammals. *Glycobiology 13*, 41R–53R.
6. Hooper, L. V., and Gordon, J. I. (2001) Glycans as legislators of host-microbial interactions: Spanning the spectrum from symbiosis to pathogenicity. *Glycobiology 11*, 1R–10R.
7. Listinsky, J. J., Siegal, G. P., and Listinsky, C. M. (1998) α-L-fucose: a potentially critical molecule in pathologic processes including neoplasia. *Am. J. Clin. Pathol. 110*, 425–440.
8. Willems, P. J., Seo, H. C., Coucke, P., Tonlorenzi, R., and O'Brien, J. S. (1999) Spectrum of mutations in fucosidosis. *Eur. J. Hum. Genet. 7*, 60–67.
9. Lowe, J. B. (2002) Glycosylation in the control of selectin counterreceptor structure and function. *Immunol. Rev. 186*, 19–36.
10. Giardina, M. G., Matarazzo, M., Morante, R., Lucariello, A., Varriale, A., Guardasole, V., and De Marco, G. (1998) Serum α-L-fucosidase activity and early detection of hepatocellular carcinoma: A prospective study of patients with cirrhosis. *Cancer 83*, 2468–2474.
11. Barker, C., Dell, A., Rogers, M., Alhadeff, J. A., and Winchester, B. (1988) Canine α-L-fucosidase in relation to the enzymic defect and storage products in canine fucosidosis. *Biochem. J. 254*, 861–868.
12. Fernandez-Rodriguez, J., Ayude, D., de La Cadena, M. P., Martinez-Zorzano, V. S., de Carlos, A., Caride-Castro, A., de Castro, G., and Rodriguez-Berrocal, F. J. (2000) α-L-fucosidase enzyme in the prediction of colorectal cancer patients at high risk of tumor recurrence. *Cancer Detect. Prev. 24*, 143–149.
13. Glick, M. C., Kothari, V. A., Liu, A., Stoykova, L. I., and Scanlin, T. F. (2001) Activity of fucosyltransferases and altered glycosylation in cystic fibrosis airway epithelial cells. *Biochimie 83*, 743–747.
14. Scanlin, T. F., and Glick, M. C. (1999) Terminal glycosylation in cystic fibrosis. *Biochim. Biophys. Acta 1455*, 241–253.
15. Wright, L. M., Kreikemerier, J. T., and Fimmel, C. J. (2007) A concise review of serum markers for hepatocellular cancer. *Cancer Detect. Prev. 31*, 35–44.
16. Yuan, K., Kucik, D., Singh, R. K., Listinsky, C. M., Listinsky, J. J., and Siegal, G. P. (2008) Alterations in human breast cancer

adhesion-motility in response to changes in cell surface glycoproteins displaying α-L-fucose moieties. *Int. J. Oncol. 32*, 797–807.
17. Butters, T. D., Scudder, P., Rotsaert, J., Petursson, S., Fleet, G. W. J., Willenbrock, F. W., and Jacob, G. S. (1991) Purification to homogeneity of *Charonia lampas* α-fucosidase by using sequential ligand-affinity chromatography. *Biochem. J. 279*, 189–195.
18. Johnson, S. W., and Alhadeff, J. A. (1991) Mammalian α-L-fucosidases. *Comp. Biochem. Physiol. 99B*, 479–488.
19. Van Hooren, P. T., and van Damme, E. J. (1999) L-Fucose: occurrence, physiological role, chemical, enzymatic and microbial synthesis. *J. Chem. Technol. Biotechnol. 74*, 479–497.
20. Sano, M., Hayakawa, K., and Kato, I. (1992) Purification and characterization of α-L-fucosidase from *Streptomyces* species. *J. Biol. Chem. 267*, 1522–1527.
21. Wong-Madden, S. T., and Landry, D. (1995) Purification and characterization of novel glycosidases from the bacterial genus *Xanthomonas*. *Glycobiology 5*, 19–28.
22. Nagae, M., Tsuchiya, A., Katayama, T., Yamamoto, K., Wakatsuki, S., and Kato, R. (2007) Structural basis of the catalytic reaction mechanism of novel 1,2-α-L-fucosidase from *Bifidobacterium bifidum*. *J. Biol. Chem. 282*, 18497–18509.
23. Watkins, P., and Alhadeff, J. A. (1981) Kinetic and immunochemical characterization of α-L-fucosidase from vertebrate livers. *Comp. Biochem. Physiol. 68B*, 509–516.
24. Alhadeff, J. A., and Janowsky, A. J. (1975) Human serum α-L-fucosidase. *Clin. Chim. Acta 82*, 133–140.
25. Alhadeff, J. A., and Andrews-Smith, G. L. (1984) Radioimmunochemical evidence for the role of carbohydrate in antigenic determinants on human liver α-L-fucosidase. *Biochem. J. 223*, 293–298.
26. Turner, B. M., Beratis, N. G., and Hirschhorn, K. (1975) Silent allele as a genetic basis of fucosidosis. *Nature 257*, 391–392.
27. Beem, E. P., Lisman, J. J. W., van Steijn, G. J., van der Wal, C. J., Trippelvitz, L. A. W., Overdijk, B., van Halbeek, H., Mutsaers, J. H. G. M., and Vliegenthart, J. F. G. (1987) Structural analysis of the carbohydrate moieties of α-L-fucosidase from human liver. *Glycoconjugate J. 4*, 33–42.
28. Argade, S. P., Hopfer, R. L., Strang, A. M., Van Halbeek, H., and Alhadeff, J. A. (1988) Structure studies on the carbohydrate moieties of human liver α-L-fucosidase. *Arch. Biochem. Biophys. 226*, 227–247.
29. Piesecki, S., and Alhadeff, J. A. (1992) The effect of carbohydrate removal on the properties of human liver α-L-fucosidase. *Biochim. Biophys. Acta 1119*, 194–200.
30. Fukushima, H., DeWet, J. R., and O'Brien, J. S. (1985) Molecular cloning of a cDNA for human α-L-fucosidase. *Proc. Natl. Acad. Sci. U.S.A. 82*, 1262–1265.
31. Occhiodoro, T., Beckman, K. R., Morris, C. P., and Hopwood, J. J. (1989) Human α-L-fucosidase: Complete coding sequence form cDNA clones. *Biochem. Biophys. Res. Commun. 164*, 439–445.
32. Kretz, K. A., Cripe, D., Carson, G. S., Fukushima, H., and O'Brien, J. S. (1992) Structure and sequence of the human α-L-fucosidase gene and pseudogene. *Genomics 12*, 276–280.
33. De Carlos, A., Montenegro, D., Alonso-Rodriguez, A., De La Cadena, M. P., Rodriguez-Berrocal, F. J., and Martinez-Zorzano, V. S. (2003) Purification of human α-L-fucosidase precursor expressed in *Escherichia coli* as a glutathione S-transferase fusion protein. *J. Chromatogr. B 786*, 7–15.
34. White, W. J., Schray, K. J., and Alhadeff, J. A. (1985) Studies on the catalytic residues at the active site of human liver α-L-Fucosidase. *Biochim. Biophys. Acta 829*, 303–310.
35. White, W. J., Jr., Schray, K. J., Legler, G., and Alhadeff, J. A. (1987) Further studies on the catalytic mechanism of human liver α-L-fucosidase. *Biochim. Biophys. Acta 912*, 132–138.
36. Eneyskaya, E. V., Kulminskaya, A. A., Kalkkinen, N., Nifantiev, N. E., Arbatskii, N. P., Saenko, A. I., Chepurnaya, O. V., Arutyunyan, A. V., Shabalin, K. A., and Neustroev, K. N. (2001) An α-L-fucosidase from *Thermus* sp. with unusually broad specificity. *Glycoconjugate J. 18*, 827–834.
37. Berteau, O., McCort, I., Goasdoue, N., Tissot, B., and Daniel, R. (2002) Characterization of a new α-L-fucosidase isolated from the marine mollusk *Pecten maximus* that catalyzes the hydrolysis of α-L-fucose from algal fucoidan (*Ascophyllum nodosum*). *Glycobiology 12*, 273–282.
38. Cobucci-Ponzano, B., Trincone, A., Giordano, A., Rossi, M., and Moracci, M. (2003) Identification of the catalytic nucleophile of the family 29 α-L-fucosidase from *Sulfolobus solfataricus* via chemical rescue of an inactive mutant. *Biochemistry 42*, 9525–9531.
39. Tarling, C. A., He, S., Sulzenbacher, G., Bignon, C., Bourne, Y., Henrissat, B., and Withers, S. G. (2003) Identification of the catalytic nucleophile of the family 29 α-L-fucosidase from *Thermotoga maritima* through trapping of a covalent glycosyl-enzyme intermediate and mutagenesis. *J. Biol. Chem. 278*, 47394–47399.
40. McCarter, J. D., and Withers, S. G. (1994) Mechanism of enzymatic glycoside hydrolysis. *Curr. Opin. Struct. Biol. 4*, 885–892.
41. Ly, H. D., and Withers, S. G. (1999) Mutagenesis of glycosidases. *Annu. Rev. Biochem. 68*, 487–522.
42. Sulzenbacher, G., Bignon, C., Nishimura, T., Tarling, C. A., Withers, S. G., Henrissat, B., and Bourne, Y. (2004) Crystal structure of *Thermotoga maritime* α-L-fucosidase. Insights into the catalytic mechanism and the molecular basis for fucosidosis. *J. Biol. Chem. 279*, 13119–13128.
43. Bairoch, A., Apweiler, R., Wu, C. H., Barker, W. C., Boeckmann, B., Ferro, S., Gasteiger, E., Huang, H., Lopez, R., Magrane, M., Martin, M. J., Natale, D. A., O'Donovan, C., Redaschi, N., and Yeh, L. S. (2005) The universal protein resource (UniProt). *Nucleic Acids Res. 33*, D154−D159.
44. Laemmli, U. K. (1970) Cleavage of structural proteins during the assembly of the head of bacteriophage T4. *Nature 227*, 680–685.
45. Gu, G., Du, Y., Hu, H., and Jin, C. (2003) Synthesis of 2-chloro-4-nitrophenyl α-L-fucopyranoside: a substrate for α-L-fucosidase (AFU). *Carbohydr. Res. 338*, 1603–1607.
46. Excoffier, G., Gagnaire, D., and Utille, J. P. (1975) Synthesis of oligosaccharides on polymeric supports. V. Selective cleavage by hydrazine of the anomeric acetyl groups of acetylated glycosyl residues. *Carbohydr. Res. 39*, 368–373.
47. Schmidt, R. R. (1986) New methods for the synthesis of glycosides and oligosaccharides—Are there alternatives to the Koenigs-Knorr method? *Angew. Chem., Int. Ed. 25*, 212–235.
48. Schmidt, R. R., Wegmann, B., and Jung, K.-H. (1991) Stereospecific synthesis of α-L-fucopyranosyl phosphates and of GDP-fucose via trichloroacetimidate. *Liebigs Ann. Chem. 2*, 121–124.
49. Leatherbarrow, R. T. (1987)EnzFitter. A non-linear regression data analysis program for IBM-PC, Elsevier Biosoft, Cambridge, U.K.
50. D'Aniello, A., Hakimi, J., Cacace, G. M., and Ceccarini, C. (1982) The purification and characterization of α-L-fucosidase from the hepatopancreas of *Octopus vulgaris*. *J. Biochem. 91*, 1073–1080.
51. Li, Y.-K., Chir, J., and Chen, F.-Y. (2001) Catalytic mechanism of a family 3 β-glucosidase and mutagenesis study on residue Asp247. *Biochem. J. 355*, 835–840.
52. Zechel, D. L., Reid, S. P., Stoll, D., Nashiru, O., Warren, R. A. J., and Withers, S. G. (2003) Mechanism, mutagenesis and chemical rescue of a β-mannosidase from *Cellulomonas fimi*. *Biochemistry 42*, 7195–7204.
53. Klimacek, M., Kavangeh, K. L., Wilson, D. K., and Nidzteky, B. (2003) On the role of Brønsted catalysis in *Pseudomonas fluorescens* mannitol 2-dehydrogenase. *Biochem. J. 375*, 141–149.
54. Wan, C.-F., Chen, W.-H., Chen, C.-T., Chang, M. D.-T., Lo, L.-C., and Li, Y.-K. (2007) Mutagenesis and mechanistic study of a glycoside hydrolase family 54 α-L-arabinofuranosidase from *Trichoderma koningii*. *Biochem. J. 401*, 551–558.
55. Sinnott, M. L. (1990) Catalytic mechanism of enzymic glycosyl transfer. *Chem. Rev. 90*, 1171–1202.
56. Zechel, D. L., and Withers, S. G. (2000) Glycosidase mechanisms: Anatomy of a finely tuned catalyst. *Acc. Chem. Res. 33*, 11–18.
57. Cobucci-Ponzano, B., Mazzone, M., Rossi, M., and Moracci, M. (2005) Probing the catalytically essential residues of α-L-fucosidase from the hyperthermophilic archaeon *Sulfolobus solfataricus*. *Biochemistry 44*, 6331–6342.
58. Vocadlo, D. J., Wicki, J., Rupitz, K., and Withers, S. G. (2002) A case for reverse protonation: identification of Glu160 as an acid/base catalyst in *Thermoanaerobacterium saccharolyticum* β-xylosidase and detailed kinetic analysis of a site-directed mutant. *Biochemistry 41*, 9736–9746.
59. Cobucci-Ponzano, B., Conte, F., Rossi, M., and Moracci, M. (2008) The α-L-fucosidase from *Sulfolobus solfataricus*. *Extremophiles 12*, 61–68.

BI801529T